

Research Article

Sol-gel preparation and study of bio-corrosion and anti-fungi behavior of TiO₂ nanostructured coating applied on mild steel

A. Shanaghi ^{*1}, H. Rezaei², A. Shanaghi³¹ Department of Materials Engineering, Faculty of Engineering, Malayer University, Malayer, Iran² Department of Soil Science, Faculty of Agriculture, Malayer University, Malayer, Iran³ Department of Electrical and Telecommunication Engineering, University of Science and Research, Tehran, Iran

ARTICLE INFO

Keywords:

TiO₂ nanostructured coating, Antifungal properties, Aspergillus niger, Aspergillus flavus, Bio-corrosion behavior, Mild steel, Sol-gel method.

Article history:

Received 08 February 2023

Received in revised form 16 October 2023

Accepted 09 March 2024

ABSTRACT

TiO₂ nanoparticle coatings have beneficial antifungal and anti-bacterial properties, which make them a reliable alternatives to resist against the occurrence and growth of viral, bacterial, parasitic or fungal infections. Such characteristic is of great importance particularly for public environments where applications such as cutting tools and hospital equipment demand strict levels of hygiene. In this article, we have successfully produced a unique TiO₂ coating on mild steel substrate by using sol-gel deposition technique to improve its corrosion resistance and anti-fungal properties. In this present investigation a uniform and TiO₂ nanostructured coating on steel substrate has been synthesized using Sol-gel method. The coating was deposited on a mild steel substrate by a dip coating technique followed by three different type of cooling rates: 1, 3 and 6 °C/min. The phase morphology, micro-structure and composition of the coatings were studied by X-ray diffraction (XRD) and field emission scanning electron microscopy (FESEM) characterization techniques. Bio-corrosion behaviour was evaluated by conducting electrochemical impedance spectroscopy and potentiodynamic polarization tests in 0.9 wt % NaCl solution at 37 °C to simulate aggressive environment. The antifungal performances of the coating have been studied on Aspergillus niger and Aspergillus flavus. The specimens Reduction of corrosion current intensity for coated specimens varies from 15.8 to 0.8 μA/cm² and shifting open circuit potential (E_{ocp}) from -1550 mV to -391 mV, for heating and cooling rate 6 and 1 °C/min, respectively. Shifting E_{ocp} towards more positive values by decreasing heating and cooling rate of heat treatment, enhanced corrosion resistance by reducing porosities and cracks in the coating. It is worthy to note that the antifungal properties TiO₂ nanostructured coating on Aspergillus niger and Aspergillus flavus are 50 and 30 % after 2 months, respectively.

1. Introduction

Nanostructured TiO₂ thin films as a protective coat-

*Corresponding author

Email: alishanaghi@gmail.com

Address: Department of Materials Engineering, Faculty of Engineering, Malayer University, Malayer, Iran.

1. Associate Professor, 2. Assistant Professor, 3. MSc. Student

<http://10.22034/IJISSI.2024.1989419.1261>

Published by ISSI (Iron & Steel Society of Iran)

ings are used in a wide range of applications, such as ultraviolet filters for optics and packing materials [1, 2], antireflection coatings for photovoltaic cells and passive solar collectors [3], photo catalysts for purification and treatment of water and air [4, 5], anodes for ion batteries [6], electro chromic displays [7], transparent conductors, self-cleaning coatings for windows and tiles [8] and antifungal layers for public environment applications[9]. It has been shown that some applications greatly benefited from a nanostructured phase for TiO₂. TiO₂ Ceramic coatings can be deposited on the substrate by several var-

ious techniques that have been developed for this purpose [10-12].

Among these techniques, sol-gel techniques are often preferred for several reasons: they are simple, low temperature (usually 200 to 600 C) techniques, which avoid possible decomposition problems; can provide high-purity, high-quality and stoichiometric coatings; the adjustment of the coating thickness can be done easily; some of them, like the dip-coating method, are suitable for coatings of complex-shaped substrates, etc.

There have been reports of severe illness cause as the result of outdoor and indoor exposures, and direct relation has been discovered between fungal contamination and illnesses such as pulmonary diseases, neurological and oncology disorders. Over 200 species of mostly asexual fungi have been found in soil as well as in foods, dust particles, organic debris and decomposed vegetation [13-16].

Several studies have proven that the grain size of TiO₂ coatings can be changed through modification of heat-treatment temperature and calculated activation energy for grain growth of metastable phase of TiO₂, which is about 23 kJ/mol. and also the heating and cooling rate of heat treatment influences the grain size and uniformity of sol-gel coating. Indeed, the heating rate can affect the uniformity and grain growth of the TiO₂ coating; while cooling rate can affect the emergence of defects in the coating. The morphology, structure and particle size of nanostructured coatings contributes to the anti-fungi property of TiO₂ coatings. According to recent research, it is essential to explore the heating and cooling rates effects on the anti-fungi property of TiO₂ coating to enhance their performance through nanocrystalline structure [17-21].

So, in this work an attempt was made to apply TiO₂ nanoparticle coating using the sol-gel technique. Structural and micro-structural characterizations of the coatings have been investigated by XRD and FESEM techniques, as well bio-corrosion behaviour was studied by electrochemical test such as electrochemical impedance spectroscopy and potentiodynamic tests in 0.9 wt % NaCl solution at 37 C°, which is an aggressive environment. The antifungal performances of the coating have been evaluated through *Aspergillus niger* and *Aspergillus flavus* methods.

2. Experimental

The reagents are used in as received conditions. Since the water content of the sol has a critical role in hydrolysis and polycondensation reactions, almost pure ethanol (Merck 99%) is used as a solvent, ethyl acetoacetat (EAcAc) (Merck 99%) used as chelating agent, tetra n-butyl orthotitanate (TBT) (Merck 98%) is used as a precursor and the final solution is prepared according to the literature [10-12, 22-24]. Dip coating with 0.5 mm/min is used

to apply sol gel coating. Before applying the coating on mild steel, the substrates must be cleaned from impurities, oxide layers and dust particles. For this reason, polishing applied with sandpaper from 600 to 4000 mesh, respectively. Then, followed by polishing with 0.1 μm diamond solution. Furthermore, steel substrates are cleaned with the ethanol in an ultrasonic bath, and dried at room temperature prior to the deposition process.

After the coating deposition on the mild steel substrates, samples were dried at 80°C for 0.5h and sintered at 500°C for 1h in order to produce dried gels. Then, three different type of heat treatment were applied on the samples in which heating and cooling rates are 1, 3 and 6 °C/min. TiO₂ coatings characterized by XRD to determine the crystallinity of the resulting bulk powdered material, X-ray diffraction (XRD) patterns are recorded on Philips PW 3040/60 X'Pert PRO, Almelo Netherlands powder diffractometer using CuK_α radiation, operating at 45 kV and 40 mA. (Philips, using CuK_α radiation $\lambda = 1.54056\text{\AA}$) and FESEM (TESCAN, MIRA3) techniques. The electrochemical behavior of coated and uncoated mild steel is investigated by means of electrochemical methods (AC and DC techniques). Electrochemical measurements are carried out at 37 C° temperature in the conventional three electrode cell, using PAR 263A potentiostat/ galvanostat and frequency response analyzer 1025 (both Princeton Applied Research, Oak Ridge, TN, USA). The reference electrode is a saturated calomel electrode (SCE), and auxiliary electrodes (platinum plate) in 250 ml of 0.9 wt % NaCl solution. The surface area was about 1 cm², while a platinum plate is used as the counter electrode. Electrochemical impedance spectroscopy (EIS) measurements are conducted in a simulated marine environment in near pH-neutral 0.9 wt at % NaCl solution 37 C° after 30 min of immersion measurements are performed with the amplitude of the voltage perturbation of 0.01 Vrms with in a frequency range of 10mHz to 100 KHz. All experiments are performed at open circuit potential.

The corrosion resistance of bare and coated mild steel is also examined in 0.9 wt at % NaCl by means of the polarization measurements of electrochemical workstation (Ivium, Netherland) comprising the working (coated mild steel), reference (saturated calomel electrode), The open circuit potential (OCP) measurement was conducted for 30 min of immersion at 37 C° in the prepared solution, the polarization curves are scanned in narrow (-250 mV vs. open circuit potential) and wide (+250 mV vs. open circuit potential) potential window. Potential scan rate is 1 mV.s-1. Data obtained in the narrow potential window are used for the determination of the polarization resistance, i.e., by using the linear polarization method, while the data obtained in the wide potential window are analyzed by the Tafel extrapolation method.

Isolates of *Aspergillus Niger*, and *Aspergillus Flavus* are obtained from Iranian science industrial research with

no: PTCC 5009 are tested for in vitro susceptibility to TiO₂ nanoparticle coatings deposited on the mild steel substrates. Dextrose Agar dilution test carried out. To perform this, 1* 10⁵ conidia of *Aspergillus* first inoculated on Zchapex Agar with 0.05 % chloramphenicol and incubated in 28 °C. After three days, the surfaces of mediums rinsed with 5 ml sterile PBS (pH=7.4) and then filtered through GFC no.4. Spores of these suspension counted with hemocytometer to be 1*10⁶ cell/ml. Subsequently, 1, 4, 6 and 8*10⁶ spore/ml added to Sabouraud, so Agar medium with 0.05% chloramphenicol yielded in 27- 35 °C. Coated mild steel slides with TiO₂ nanoparticle deposited on medium separately and incubated for 3-60 days.

3. Result and Discussion

3.1. Coatings Characterization

Fig. 1. shows XRD spectrum of TiO₂ nanoparticle coating. According to the standard card (JCPDS no.: 84-1286 and 88-1175), the XRD spectrum indicates strong diffraction peaks of anatase phase. It shows anatase is the major phase of the coating and there is not any another phase in the coating, so there is not any stress in the structure and anatase (101) and rutile (110) reflections can be seen at 25.3° and 27.6° in Fig. 2. [23, 24].

According to other studies, photocatalyst and antibacterial of anatase phase of TiO₂ is more than rutile phase [17-21]. These results agree with thermodynamic and heat treatment properties of titanium oxide in 500 °C, and also decreasing heating and cooling rate resulted in the expansion of the main peak and indicates the peak related to the rutile phase.

Fig. 2. shows FESEM images and cross section im-

age of TiO₂ nanostructured coatings. Each of heating and cooling rate such as 1, 3 and 6 °C/min has led to coatings with different morphology. Actually, increasing heating and cooling rate led to decrease the particle size of TiO₂ cluster and introduced defects such as cracks and holes to the coating. One of important contributor to the antifungal property are grain size and distribution of rutile and anatase phases. Note that, smaller particles have higher surface areas and particle numbers per unit mass, and this may contribute to the higher antifungal activity observed in this study. Similar studies have shown that smaller particles caused significant reduction in cell viability due to a larger contact surface area, and therefore have a higher tendency to induce oxidative damage, causing more cell death [23].

Another essential factor to control the grain size and distribution in the TiO₂ coatings, which are deposited by sol-gel technique is the heat treatment. Different cooling or heating rates induce different characteristics to the performance of the TiO₂ coatings [24, 25]. The molar ratio of precursors to other additives of the solution is important. Figs. 2a-b. exhibits that, a uniform and fine grain sized TiO₂ nanostructured coating with less cracks achieved with heat treatment with heating and cooling rate of 1 °C/min, but Figs. 2c-f. indicate some cracks and defects on the TiO₂ nanostructured coating for heating and cooling rate of 3 and 6 °C/min. Actually, increasing heating and cooling rates accelerates the evaporation of fugitive materials from sol-gel coatings, which leave certain amount of defects in the coatings. However, homogeneous, crack-free and uniform coatings with thicknesses of 800–900 nm produced at heating and cooling rate of 1 °C/min (Fig. 2g.).

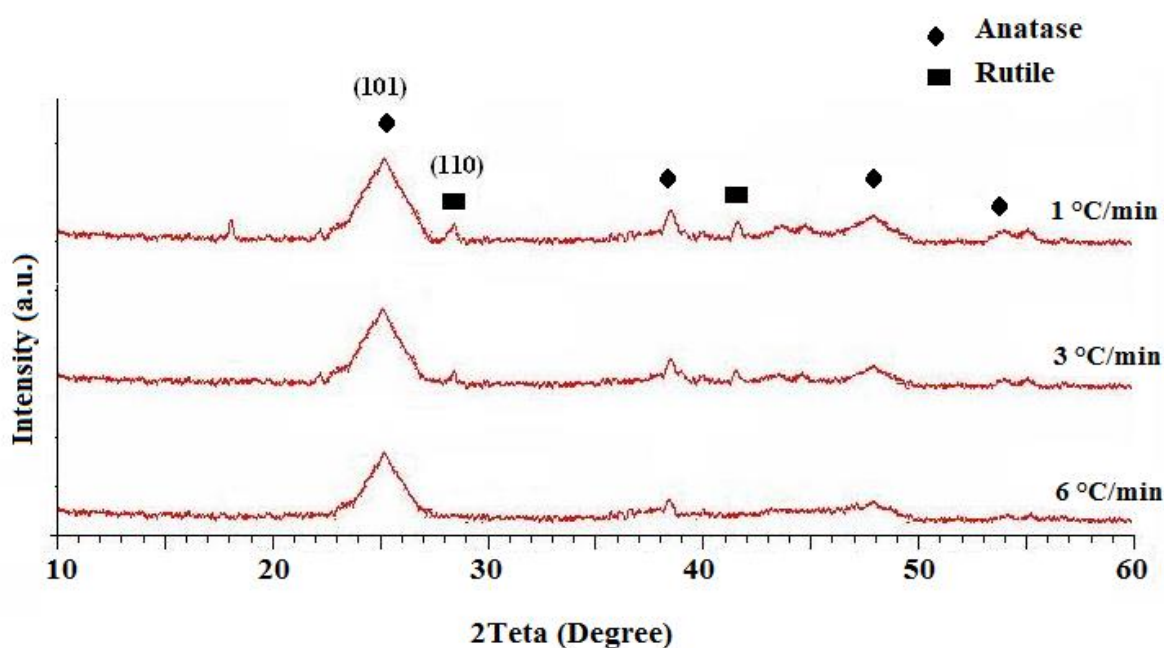


Fig. 1. XRD diffraction curves of TiO₂ coatings on mild steel substrates with three different heating and cooling rate such as 1, 3 and 6 °C/min.

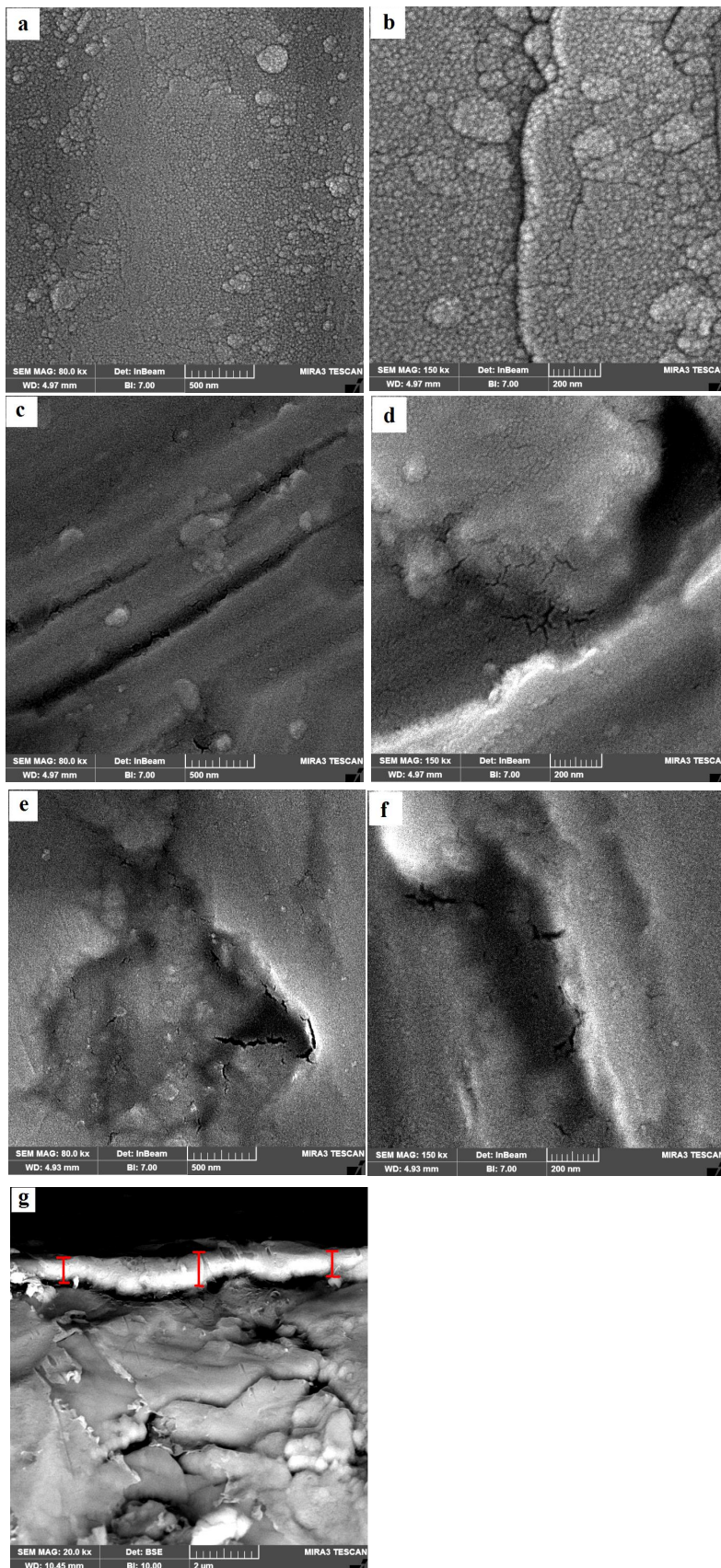


Fig. 2. FESEM image of TiO₂ nanoparticle coating with two different magnifications such as, 80 KX and 150 KX for different heating and cooling rate of: (a-b) 1 C°/min, (c-d) 3C°/min, and (e-f) 6 C°/min; and (g) cross section image of TiO₂ nanoparticle coating.

According to results of XRD and FESEM, the TiO_2 nanoparticle sizes varies from 40 – 60nm for different heating and cooling rates such as 6, 3 and 1 °C/min.

3.2. Corrosion behaviour

Open circuit voltage V_{oc} (V/RHE) monitoring and polarization of the TiO_2 nanostructured coatings allows the assessment of the corrosion protection of mild steel substrates in a corrosive solution.

Fig. 3. illustrates the OCP plots for bare mild steel and TiO_2 nanostructured coating on mild steel at three different heating and cooling rates of 1, 3 and 6 °C/min at 1400 s of immersion time in 9 wt% NaCl solution to simulate and aggressive environment, which indicates the TiO_2 nanostructured coating, which was heat treated by rate of 1 °C/min has a lower tendency to perform corrosion reactions compared to other samples, as well, increasing immersion time led to moving towards positive of its potential value. This phenomenon can be due to gradual deposition of corrosion products, and reduction of anodic and cathodic active sites on the surface of the TiO_2 nanostructured coating. But negative slop of potential in the early stages of others samples can be due to the penetration of soluble aggressive ions such as Cl^- ions through the porosities of the TiO_2 nanostructured coating into the coating, which leads to increased intensity of substrate dissolution reaction, and toward the potential amount to more negative values. Because of more positive potential, the titanium oxide nanostructure coating is heat treated by rate of 1 °C/min has more corrosion resistance and less tendencies to corrosion reactions [25, 26].

Fig. 4. Demonstrates an investigation of charge transfer resistance of nano-structured TiO_2 at different ionic strength, where the The nyquist, bode and bode- phase plots of bare mild steel and TiO_2 nanostructured coatings with three different heating and cooling rate such as 1, 3 and 6 °C/min in 9 wt% in NaCl solution at 37 °C are shown. According to the Fig. 4. Nyquist curves have two time constants at high and low frequencies, which are due to the titanium oxide layer at high frequencies and the double

layer at the interface between the sample and the 9 wt% NaCl solution at low frequencies, respectively. The titania nanostructured coating was heat-treated at rates of 1 and 3 °C/min exhibited a larger oxide semi-circle at high frequency compared to the semi-circle formed at low frequencies, which indicates the formation of a stable titanium oxide layer [25-28]. But heating and cooling rate 6 °C/min cause to the diameter of the first semi-circle to decreases at high frequencies, which could indicate electrolyte uptake and penetration through defects and surface porosities of the titanium oxide coating. Increasing the phase angle and broadening the bode-phase oxide coating curve of 1 °C/min indicate its better performance and stability compared to other coatings.

The mechanism and corrosion behavior of the coating were studied by using electrical equivalent circuits for an electrochemical cell, which will include a specific combination of resistors and capacitors [26-29]. The proposed electrical equivalent circuits for bare mild steel and TiO_2 nanostructured coatings are shown in Fig. 5. and the results are summarized in Table 1. R_{coat} and CPE_{coat} represent the resistance and capacitance of the titanium oxide coating, respectively, R_{ct} and CPE_{dl} are the charge transfer resistance and dual layer capacity, n_{dl} is the associated coefficient and R_s is the solution resistance of 0.9 wt% NaCl solution at 37 °C. To indicate the validity and accuracy of the proposed electrical equivalent circuits, Chi-squared is used, the value of which indicates the very high compliance of the proposed electrical equivalent circuits with the plots obtained from the impedance test. The nyquist curves and R_{coat} values indicate the proper performance of the titania nanostructured coating heat- treated by rate 1 °C/min, as well penetration as of corrosive ions and water causing the decrease of R_{ct} with rising heating and cooling rate. This behavior could be confirmed by the coating capacitance value of 6 °C/min, which is as a criterion for water penetration into the coating. Finally, decreasing the n_{coat} at high heating and cooling rates indicates an increase in surface roughness or changes in corrosion behavior from uniform to local states [26-29].

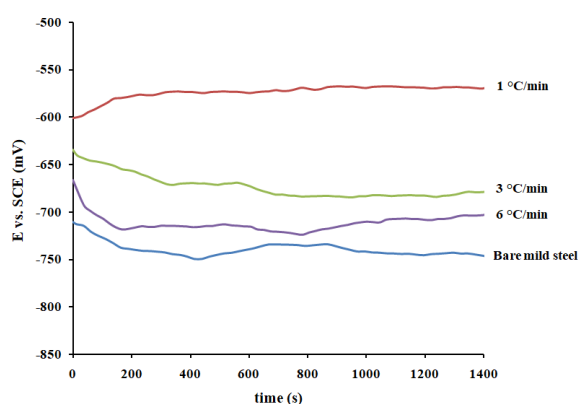


Fig. 3. E-t plots of bare mild steel and TiO_2 nanostructured coating on mild steel at three different heating and cooling rate such as 1, 3 and 6 °C/min at 1400 s of immersion time in 9 wt% NaCl solution.

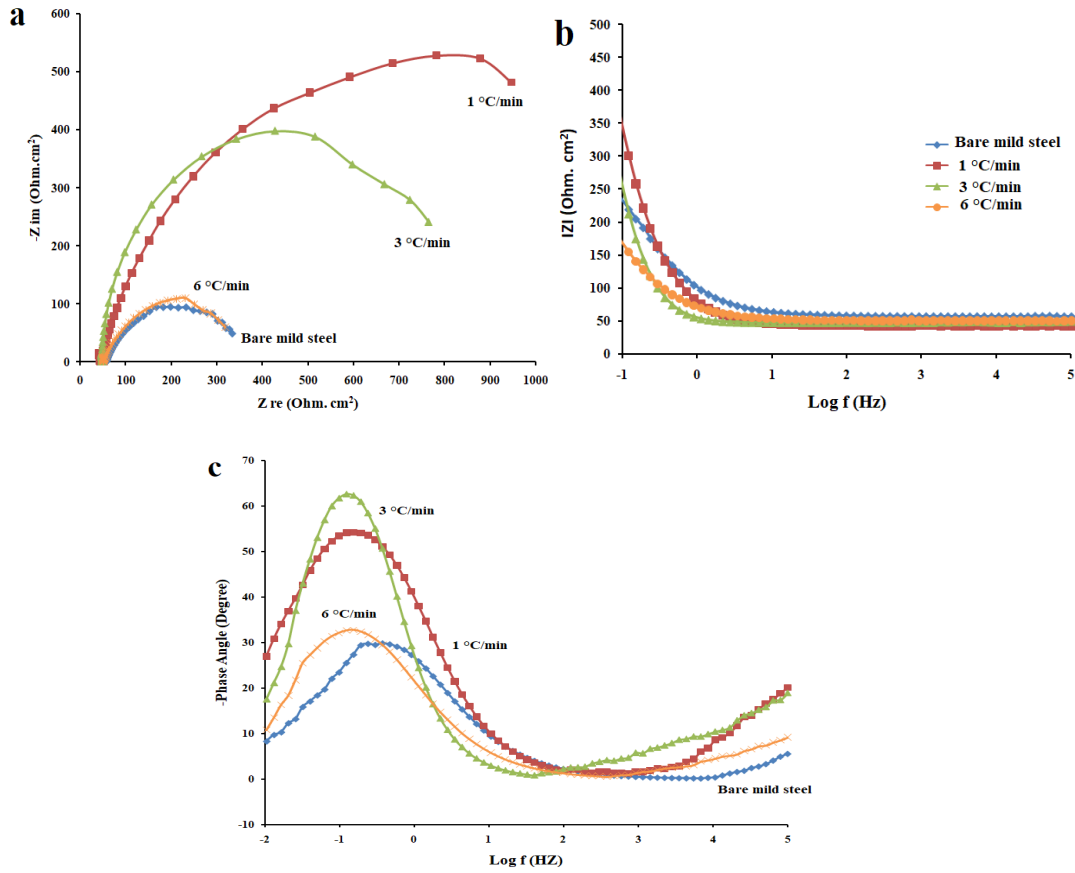


Fig. 4. a) Nyquist plots, and b-c) Bode and Bode- Phase plots of bare mild steel and TiO₂ nanostructured coating at three different heating and cooling rate such as 1, 3 and 6 C°/min in 9 wt% NaCl solution at 37 C°.

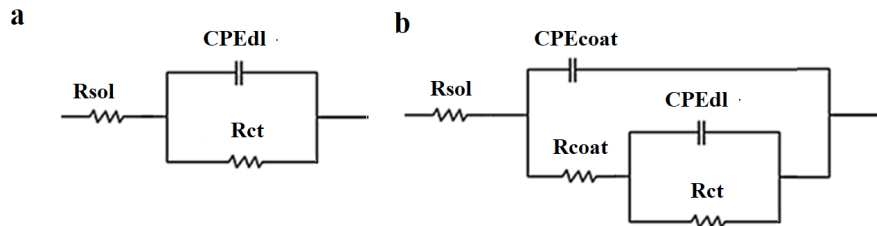


Fig. 5. Electrical equivalent circuits for, a) bare mild steel, b) TiO₂ nanostructured coatings after immersion in 0.9 wt% NaCl solution at 37 C°.

Table 1. EIS analysis parameters of bare mild steel and TiO₂ nanostructured coating on mild steel at three different heating and cooling rate such as 1, 3 and 6 C°/min after immersion in 0.9 wt% NaCl solution at 37 C°.

Samples	Heating and cooling rate (°C/min)	R _{sol} (Ω.Cm ²)	R _{coating} (Ω.Cm ²)	CPE _{coating} (μF.cm ⁻² .s ⁿ⁻¹)	n _{coating}	R _{ct} (Ω.Cm ²)	CPE _{dl} (μF.cm ⁻² .s ⁿ⁻¹)	n _{dl}	Chi-Squared
Bare Mild steel	-	47	-	-	-	312	44.7	0.87	0.00048
TiO ₂ nanostructured coating	1	53	857.2	39.4	0.99	542	410.8	0.81	0.001853
	3	38	361.4	28.1	0.91	486	487.2	0.83	0.000856
	6	42	52.9	18.3	0.83	326	496.3	0.72	0.000672

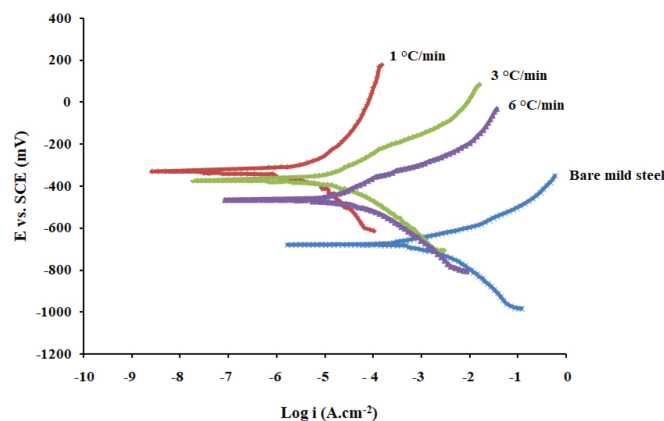


Fig. 6. Potentiodynamic curves of parameters for bare mild steel and TiO₂ nanostructured coating on mild steel at three different heating and cooling rate such as 1, 3 and 6 C°/min after immersion in 0.9 wt% NaCl solution.

Table 2. Polarization analysis parameters after immersion in 0.9 wt % NaCl solution at 37 C°.

Samples	Bare Mild steel	TiO ₂ nanostructured coating at three different heating and cooling rates (C°/min)		
		1	3	6
i_{corr} ($\mu\text{A}/\text{cm}^2$)	51.4	0.8	5.1	15.8
E_{corr} (mV)	-679	-329	-374	-464

Potentiodynamic curves of parameters for bare mild steel and TiO₂ nanostructured coating on mild steel at three different heating and cooling rates of 1, 3 and 6 C°/min after immersion in 0.9 wt% NaCl solution is shown in Fig. 6. and their results are summarized in Table 2. Reduction of corrosion current intensity from 15.8 to 0.8 $\mu\text{A}/\text{cm}^2$ and shifting open circuit potential (E_{ocp}) from -1550 mV to -391 mV, for heating and cooling rates of 6 and 1 C°/min, respectively. However, shifting E_{ocp} towards more positive values by decreasing heating and cooling rate of heat treatment, enhanced corrosion resistance by diminishing porosities and cracks in the coating, which were confirmed by FESEM results (Fig. 2.). As a result, the TiO₂ nanostructured coating, which was heat treated by heating and cooling rate of 1 C°/min, was selected as a suitable TiO₂ coating resistant, then the anti-fungal behavior was evaluated in continues.

3.3. Anti-fungal characterization

The antibacterial mechanism of nano-TiO₂ nanoparticles is a consequence of the indirect reaction between the nano-TiO₂ and cells. That means that, the reaction of photo generated electrons, photo generated holes with

water or dissolved oxygen in water forms reactive oxygen species (ROS), such as hydrogen oxygen free radicals and hydrogen peroxide free radicals, and produces chemically active hydroxyl groups and hydroxyl groups through redox reaction supercations, among others. The mechanism for bactericidal activity of TiO₂ nanoparticles is shown in Fig. 3. Active hydroxyl groups and supercations can react with biological macromolecules, such as lipids, proteins and enzymes, thereby directly damaging or destroying the structure of biological cells, such as bacteria, through a series of oxidation chain reactions, to achieve an antibacterial effect.

The obtained results confirmed that the nano-TiO₂ coated nanoparticles specimens with glass substrates has inhibitory effect at concentration of 1,4,6 and 8x10⁶ cell/ml at 27 C° on *Aspergillus* species. The specimens inhibited the growth of all examined fungi in a dose-dependent manner. The slides could inhibit 50% of the growth of *Aspergillus nigger* and 30% of the growth of *Aspergillus felavus* at concentration of 8 x 10⁸ spore/ml after 2 months, which is summarized in Table 3. In vitro activities of a known antifungal drug (AMP-B) are tested against these *Aspergillus* species at concentration of 0.3 mg/ml.

According to Table 3. it is evident that, using nano-

structured coating can increase the specific surface of the coating and enhance contact between coating and solution, and consequently increasing the efficiency of some reactions, contributing to anti-fungal reactions performance. Also nanoparticle can cover surface of the mild steel completely and leading to decreasing defects in the coating, resulting in better uniformity of anti-fungal properties of TiO₂ nanostructured coating. On the other hand, anti-fungi directly depended on types and quality

of the coating, which is applied on the glass slide substrates by sol-gel method. TiO₂ nanostructured coating enhanced the surface morphology and homogeneity of the coating and led to improvement in the efficiency and uniformity of anti-fungal performance. The uniformity and defect free surface led to enhancing anti-fungi behaviour of TiO₂ nanostructured coatings after two months compare than other coatings. These results are presented schematically by (Figs. 7 and 8.).

Table 3. Growth inhibitory of TiO₂ nanostructured coating at different concentration of *Aspergillus niger* and *Aspergillus flavus*.

Concentration of cell (cell/ml)	Heating and cooling rate (C°/min)	Growth inhibitory (%) (3 days)		Growth inhibitory (%) (2 months)	
		Aspergillus niger	Aspergillus flavus	Aspergillus niger	Aspergillus flavus
1 x10 ⁶	6	53	32	51	32
	3	53	33	50	33
	1	53	32	50	31
4 x10 ⁶	6	58	43	55	54
	3	58	43	54	54
	1	57	43	54	52
6 x10 ⁶	6	55	37	53	35
	3	54	36	53	35
	1	54	35	53	34
8 x10 ⁶	6	51	30	49	29
	3	50	30	49	29
	1	49	29	50	30

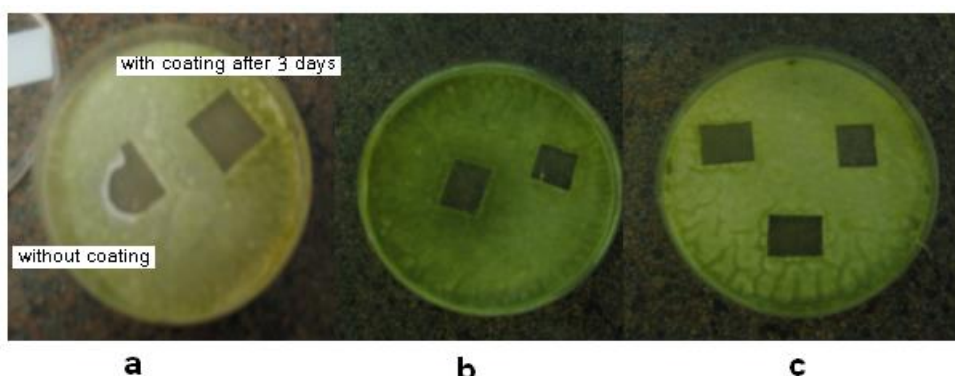


Fig. 7. Images of anti-fungi test of TiO₂ nanostructured coating and mild steel for *Aspergillus flavus*: (a) without coating and 3 days; and Images of anti-fungi test of TiO₂ nanoparticle coating for *Aspergillus flavus*: (b) 3 days, and (c) 2 months.

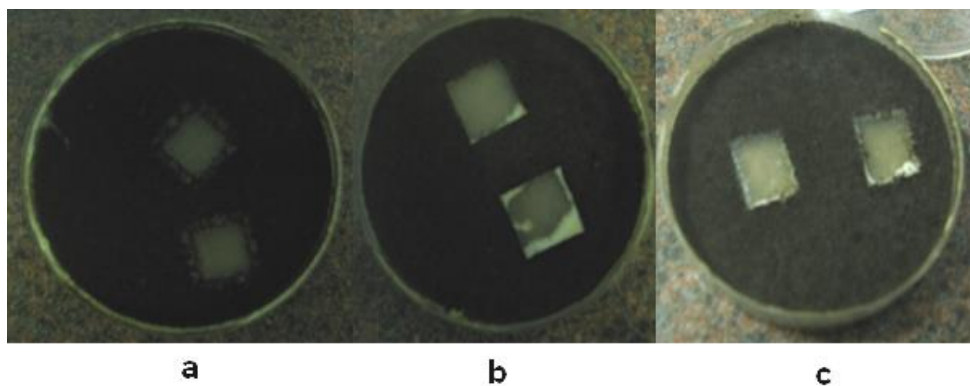


Fig. 8. Picture of anti-fungi test of TiO_2 nanostructured coating for *Aspergillus niger* (a) without coating, (b) 3 days, (c) 2 months.

It was observed that the TiO_2 nanostructured coating contributed to the prevention of the fungi growth, and their properties were remained steady after 2 months trial period while no considerable growth of fungi in the coating was observed during this course of time period.

4. Conclusions

TiO_2 nanoparticle coating with convenient homogeneity and uniformity was deposited on mild steel substrate through sol-gel deposition technique. Reduction of corrosion current intensity from 15.8 to 0.8 $\mu\text{A}/\text{cm}^2$ and shifting open circuit potential (E_{ocp}) from -1550 mV to -391 mV, for heating and cooling rate 6 and 1 $^\circ\text{C}/\text{min}$ are witnessed, respectively. As a result, shifting E_{ocp} towards more positive values by decreasing heating and cooling rate of heat treatment, enhanced corrosion resistance by diminishing porosities and cracks in the TiO_2 nanoparticle coating. Also, the Agar dilution method can accurately determine the susceptibility of fungi against antifungal agents. At the current research antifungal properties of TiO_2 nanoparticle coating deposited on mild steel substrate were evaluated through MIC method. Different concentrations of *Aspergillum* species were suspended in sabouraud and dextrose Agar in the presence of TiO_2 nanoparticle deposited on glass substrate. The maximum inhibitory effect of powders was discovered to be in the range of 4×10^6 - 6×10^6 for all tested *Aspergilla*. The MFC values of these coated glass substrates were measured at concentration of 8×10^6 cell/ml. Accordingly, TiO_2 nanostructured coating showed better antifungal activities against two *Aspergillum* species. It is clear that, using TiO_2 nanoparticles enhanced the surface morphology and homogeneity of the deposited coatings. Also, heat treatments of the specimens proved that the low heating and cooling rate of 1 $^\circ\text{C}/\text{min}$, decreases defects in the coatings and increases grain size, leading to the development of a efficient and uniform anti-fungal product.

References

[1] Bonini N, Carotta M.C, Chiorini A, Guidi V, Malagu

C, Martinelli G, Paglialonga L, Sacerdoti M, Doping of a nanostructured titania thick film : structural and electrical investigations Sens, Actuators B : Chem. 2000; 68: 274-280.

[2] Ivanova T, Harizanova A, Surtchev M, Nenova Z, Investigation of sol-gel derived thin films of titanium dioxide doped with vanadium oxide. Sol. Energy Mater. Sol. Cells. 2003; 76: 591-598.

[3] Perera V.P.S, Jayaweera P.V.V, Pitigala P.K.D.D.P, Andaranayake P.K.M.B, Hastings G, Perera A.G.U, Tennakone K, Construction of a photovoltaic device by deposition of thin films of the conducting polymer polythiocyanogen. Synth, Met. 2004; 143: 283-287.

[4] Keshmiri M, Mohseni M, Troczynski T, Development of novel TiO_2 sol-gel-derived composite and its photocatalytic activities for trichloroethylene oxidation, Appl, Catal. B: Environ. 2004; 53: 209-219.

[5] Mao D, Lu G, Chen Q, Influence of calcination temperature and preparation method of TiO_2 - ZrO_2 on conversion of cyclohexanone oxime to ϵ -caprolactam over $\text{B}_2\text{O}_3/\text{TiO}_2$ - ZrO_2 catalyst. Appl. Catal. A: Gen. 2004; 263: 83-89.

[6] Huang S.Y, Kavan L, Exnar I, Gratzel M.J, Rocking chair lithium battery based on nanocrystalline TiO_2 anatase, Electrochem, Soc. 1995; 142: L142-L144.

[7] Aliev A.E, Shin H.W, Image diffusion and cross-talk in passive matrix electrochromic displays, Displays. 2002; 23: 239-247.

[8] Fretwell R, Douglas P, An active, robust and transparent nanocrystalline anatase TiO_2 thin film preparation, characterisation and the kinetics of photodegradation of model pollutants, Photochem. J, Photobiol, A: Chem. 2001; 143: 229-240.

[9] Maneerat C, Hayata Y, Antifungal Activity of TiO_2 Photocatalysis against *Penicillium expansum* in Vitro and in Fruit Tests, J. Food Microbiology. 2006; 107: 99-103.

[10] Sberveglieri G, Depero L.E, Ferroni M, Guidi V, Martinelli G, Nelli P, Perego C, Sangaletti L, Mo-W-O thin films for CO sensing. Adv, Mater. 1996; 8: 334.

[11] Bally A.R, Korobeinikova E.N, Schmid P.E, Lévy F, Bussy F, Structural and electrical properties of Fe-doped

- TiO₂ thin films, *J. Phys., D. Appl. Phys.* 1998; 31: 1149.
- [12] Carotta M.C, Ferroni M, Guidi V, Martinelli G, Preparation and Characterization of Nanostructured Titania Thick Films, *Adv, Mater.* 1999; 11: 943-946.
- [13] Anaissie E. J, Mcginnis M. R, Pfaller M. A, Clinical mycology, Elsevier Health Sciences. 2009; 450.
- [14] Goldman C.H, Osmani S.A, The Aspergilli genomic, Medical aspects, biotechnology, and research methods, Taylor and Francis Group. 2008.
- [15] Llop C, Pujol I, Aguiar C, Sala J, Riba D, Guarro J, Comparison of Three Methods of Determining MICs for Filamentous Fungi Using Different End Point Criteria and Incubation Periods, *Antimicrob, Agents, Chemother.* 2000; 44: 239-242.
- [16] Martin- Mazuelos E, Peman J, Valverde A, Chaves M, Serrano M.C, Cantón E, Comparison of the Sensitivity YeastOne colorimetric antifungal panel and Etest with the NCCLS M38-A method to determine the activity of amphotericin B and itraconazole against clinical isolates of *Aspergillus* spp, *J. Antimicrob, Chemother.* 2003; 52: 365-370.
- [17] Akkaya Arter Ü.Ö, Tepehan F.Z, Influence of heat treatment on the particle size of nanobrookite TiO₂ thin films produced by sol-gel method, *Surf, Coat, Technol.* 2011; 206: 37-42.
- [18] Sun R, Chen Z, Peng J, Zheng T, The effect mechanisms of pH, complexant and calcination temperature on the hydrophilicity of TiO₂ films prepared by the sol-gel method, *Appl, Surf, Sci.* 2018; 462: 480-488.
- [19] Venkatachalam N, Palanichamy M, Murugesan V, Sol-gel preparation and characterization of nanosize TiO₂: Its photocatalytic performance, *Mater, Chem, Phys.* 2007; 104: 454-459.
- [20] Sharifiyan M.S, Shanaghi A, Moradi H, Chu P.K, Effects of high concentration of Benzotriazole on corrosion behavior of nanostructured titania-alumina composite coating deposited on Al 2024 by sol-gel method, *Surf, Coat, Technol.* 2017; 321: 36-44.
- [21] Mechiakh R, Bensaha R, Variation of the structural and optical properties of sol-gel TiO₂ thin films with different treatment temperatures Variation des propriétés structurales et optiques des couches minces de TiO₂ obtenues par voie sol-gel à différentes températures de recuit, *C. R. Phys.* 2006; 7: 464-470.
- [22] Shen G.X, Chen Y.C, Lin C.J, Corrosion protection of 316 L stainless steel by a TiO₂ nanoparticle coating prepared by sol-gel method, *Thin Solid Films.* 2005; 489: 130-136.
- [23] Ahmad N.S, Abdullah N, Yasin F.M, Antifungal activity of titanium dioxide nanoparticles against *Candida albicans*, *Bio.Res.* 2019; 14(4): 8866-8878.
- [24] Shanaghi A, Sabour Rouhaghdam A.R, Shahrabi T, Khazraii M.A, Study of TiO₂ nanoparticle coatings by the sol-gel method for corrosion protection, *Mater, Sci.* 2008; 44: 233-247.
- [25] Shanaghi A, Sabour Rouhaghdam A.R, Shahrabi T, Khazraii M.A, Corrosion protection of mild steel by applying TiO₂ nanoparticle coating via sol-gel method, *Prot. Met, Phys, Chem, Surf.* 2009; 45: 305-311.
- [26] Shanaghi A, Ahangarani S, Sabour Rouhaghdam A.R, Chu P.K, Improved tribological properties of TiC with porous nanostructured TiO₂ intermediate layer, *Mater, Chem, Phys.* 2011; 131: 420-424.
- [27] Simbar A.R, Shanaghi A, Moradi H, Chu P.K, Corrosion behavior of functionally graded and self-healing nanostructured TiO₂ - Al₂O₃ - Benzotriazole coatings deposited on AA 2024-T3 by the sol-gel method, *Mater, Chem. Phys.* 2020; 240: 122233.
- [28] Shanaghi A, Souri A.R, Chu P.K, EIS and noise study of zirconia-alumina- benzotriazole nano-composite coating applied on Al2024 by the sol-gel method, *J. Alloys Compd.* 2020; 816: 152662.
- [29] Ghafari A, Yousefpour M, Shanaghi A, Corrosion protection determine of ZrO₂/AA7057 nanocomposite coating with inhibitor using a mathematical ranking methods, *Appl, Surf, Sci.* 2019; 465: 427-439.